Magnetically induced ferroelectricity in Bi2CuO4

Zhao, L.; Guo, H.; Schmidt, W.; Nemkovski, K.; Mostovoy, M.; Komarek, A. C.

Published in:
Physical Review. B: Condensed Matter and Materials Physics

DOI:
10.1103/PhysRevB.96.054424

Publication date:
2017

Magnetically induced ferroelectricity in Bi_2CuO_4

L. Zhao,[1] H. Guo,[1] W. Schmidt,[2,3] K. Nemkovski,[4] M. Mostovoy,[5] and A. C. Komarek[1,*]

[1]*Max-Planck Institute for Chemical Physics of Solids, Nöthnitzer Str. 40, D-01187 Dresden, Germany*

[2]*Institut Laue-Langevin (ILL), CS 20156, 71 avenue des Martyrs, F-38042 Grenoble, France*

[3]*Jülich Centre for Neutron Science JCNS, Forschungszentrum Jülich GmbH, Outstation at ILL, CS 20156, 71 avenue des Martyrs, F-38042 Grenoble, France*

[4]*Jülich Centre for Neutron Science JCNS at Heinz Maier-Leibnitz Zentrum (MLZ), Forschungszentrum Jülich GmbH, Lichtenbergstraße 1, 85748 Garching, Germany*

[5]*Zernike Institute for Advanced Materials, University of Groningen, Nijenborgh 4, Groningen 9747 AG, The Netherlands*

(Received 6 March 2017; revised manuscript received 6 July 2017; published 18 August 2017)

The tetragonal copper oxide Bi_2CuO_4 has an unusual crystal structure with a three-dimensional network of well separated CuO_4 plaquettes. The spin structure of Bi_2CuO_4 in the magnetically ordered state below $T_N \sim 43$ K remains controversial. Here we present the results of detailed studies of specific heat, magnetic, and dielectric properties of Bi_2CuO_4 single crystals grown by the floating zone technique, combined with the polarized neutron scattering and high-resolution x-ray measurements. Down to 3.5 K our polarized neutron scattering measurements reveal ordered magnetic Cu moments which are aligned within the *ab* plane. Below the onset of the long range antiferromagnetic ordering we observe an electric polarization induced by an applied magnetic field, which indicates inversion symmetry breaking by the ordered state of Cu spins. For the magnetic field applied perpendicular to the tetragonal axis, the spin-induced ferroelectricity is explained in terms of the linear magnetoelectric effect that occurs in a metastable magnetic state. A relatively small electric polarization induced by the field parallel to the tetragonal axis may indicate a more complex magnetic ordering in Bi_2CuO_4.

DOI: 10.1103/PhysRevB.96.054424

I. INTRODUCTION

The discovery of high-temperature superconducting (HTSC) cuprates triggered an extensive research on copper-based materials, especially, low-dimensional cuprates with novel physical properties [1]. Among these materials, Bi_2CuO_4 is of special interest: its "2-1-4" chemical formula is common to the prototypical HTSC $R_2CuO_{4+\delta}$ compounds (R = rare earth, etc.). However, the isovalent substitution of the rare earth R^{3+} ions by Bi^{3+} ions of similar ionic size results in a different and unique crystal structure shown in Fig. 1. This difference might be caused by a strong covalent Bi-O bonding [2]. Bi_2CuO_4 has a tetragonal structure (space group $P4/ncc$), in which the Cu^{2+} ions exhibit a square-planar coordination by four oxygen ions. While in other cuprates the CuO_4 units form infinite two-dimensional CuO_2 layers (e.g., in $R_2CuO_{4+\delta}$ [1]) or quasi-one-dimensional ribbons or ladders, as in $LiCu_2O_2$ [3] or $Sr_3Ca_{11}Cu_{24}O_{41}$ [4], the CuO_4 plaquettes in Bi_2CuO_4 are isolated from each other. As shown in Fig. 1, the CuO_4 plaquettes are staggered along the c direction. Each plaquette is twisted with respect to the adjacent one with a twist/rotation angle of $\sim 33^\circ$, thus, forming chains in the c direction. These chains are separated by nonmagnetic Bi^{3+} ions. The Cu-Cu distance along the chains is of the order of 3 Å, which is larger than in copper metal. Nuclear quadrupole resonance (NQR) experiments [5] indicate that the Bi^{3+} ions are involved in the superexchange between Cu ions, i.e., Cu^{2+}-O^{2-}-Bi^{3+}-O^{2-}-Cu^{2+} paths yield long range antiferromagnetic (AFM) ordering below the Néel temperature $T_N \sim 43$ K.

First studies of the magnetic properties of Bi_2CuO_4 suggested a quasi-1D spin-1/2 chain model with possible spin dimerizaton [6]. However, neutron diffraction measurements [7–11] revealed a long range three-dimensional (3D) AFM order of C type: in the magnetic unit cell, which coincides with the chemical one, spins in chains are parallel, while spins in neighboring chains are antiparallel. However, the orientation of Cu spins was not unambiguously determined and two magnetic structures were proposed—one with spins parallel to the c axis [7,10] and one with spins within the ab plane [11]. Optical spectroscopy experiments including polarized far-infrared and Raman spectra on single crystals suggest the c axis orientation of copper spins [12–15]. Specific heat and thermal expansion studies of the critical behavior around T_N are consistent with the 3D Ising universality class, thus also suggesting an easy c axis anisotropy [16]. However, other experimental studies, including the high field anisotropic antiferromagnetic resonance (AFMR) [17–19] and torque magnetometry measurements [20], support an easy plane anisotropy in Bi_2CuO_4. Theoretical band structure calculations provided conflicting predictions [21,22]. Despite many efforts, this issue remains controversial.

Spin excitations in Bi_2CuO_4 have been investigated by inelastic neutron scattering [23,24]. The magnon dispersion spectrum can be fitted using the spin wave theory with up to four AFM exchange terms. In Ref. [24] both intrachain and interchain exchange interactions were found to be antiferromagnetic, which indicates magnetic frustration in Bi_2CuO_4.

Previous analysis of the photoelectron spectra shows that Bi_2CuO_4 is a charge-transfer insulator with a large band gap (around 2 eV) [25]. The high resistivity prevents a transport study on Bi_2CuO_4 at low temperature. Dc conductivity measurements are only feasible at temperatures far above T_N [26]. Hence dielectric or ac conductivity measurements seem

*komarek@cpfs.mpg.de

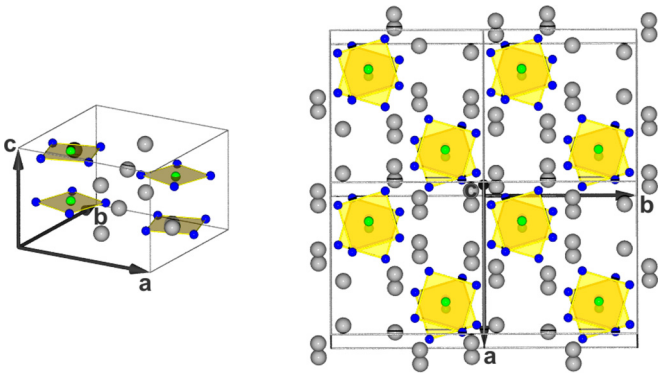

FIG. 1. Crystal structure of Bi_2CuO_4; green/blue/gray spheres denote Cu/O/Bi atoms.

to be better suited to study Bi_2CuO_4. The temperature and frequency dependent dielectric response may yield further information of microscopic physical properties of Bi_2CuO_4. However, so far, there exists only one report of the dielectric properties of Bi_2CuO_4 in the temperature range from 100 K to 300 K which is well above T_N [27].

The discovery of giant magnetoelectric effects in multiferroic manganites with coupled magnetic and electric dipoles [28,29] attracted a lot of interest in multiferroic and magnetoelectric materials. The spontaneous electric polarization observed in these frustrated magnets is induced by complex spiral spin structures which break time reversal and inversion symmetries. These unusual magnetic states are highly susceptible to applied magnetic fields, allowing for the magnetic control of electric polarization and, in some cases, for the electric control of magnetization, which is of great importance both for fundamental physics and technological applications [30,31]. A similar control can be achieved in materials showing a linear magnetoelectric effect, such as Cr_2O_3, where an electric polarization is induced by an applied magnetic field and vice versa [32–34]. The linear magnetoelectric effect also requires simultaneous breaking of time-reversal and inversion symmetry, but is usually observed in magnets with $k = 0$ magnetic states.

Copper oxides provide a rich playground for studies of magnetoelectric phenomena. The ferroelectricity induced by spin spirals was observed in the multiferroic Cu-chain compounds, $LiCu_2O_2$ and $LiCuVO_4$ [35–37], as well as in the three-dimensional CuO with a high spin ordering temperature [38]. Magnetically induced ferroelectricity and the linear magnetic response were recently observed in the spiral and skyrmion phases of the chiral cubic magnet Cu_2OSeO_3 [39,40].

Here, we systematically investigate anisotropic physical properties of floating-zone grown Bi_2CuO_4 single crystals including magnetic susceptibility, magnetization, specific heat, polarized neutron, dielectric constant, and pyroelectric measurements. Although the $k = 0$ AFM spin structure in Bi_2CuO_4 was established decades ago, it was not noticed before that it breaks inversion symmetry and thus can give rise to magnetoelectric phenomena. We report the observation of the field-induced ferroelectricity in Bi_2CuO_4, which we associate with the linear magnetoelectric effect in a metastable state.

II. EXPERIMENT

The growth of Bi_2CuO_4 single crystals was carried out in an optical floating zone furnace equipped with four elliptical mirrors (Crystal Systems Corp.). The polycrystalline rods were prepared from appropriate mixtures of Bi_2O_3 and CuO with high purities. The mixed starting materials were sintered in air at 725 °C for 72 h with several intermediate grindings. Finally, the obtained powder was pressed into a rod with ∼7 mm in diameter and ∼12 cm in length under a hydrostatic pressure of ∼60 MPa. Afterwards, the rod was sintered at 750 °C for 24 h. During the floating zone growth the crystal was grown in a pure oxygen atmosphere. Due to the low surface tension, the molten zone of the Bi_2CuO_4 is difficult to control. In literature [41] fast growth rates (10 mm/h) were reported in order to cope with the low surface tension of the Bi_2CuO_4 melt. With such a growth speed, the quality of our single crystals was not good. However, by lowering the growth speed to 3 mm/h and carefully controlling the molten zone we, finally, obtained well crystalized single crystals (as confirmed by Laue diffraction) with typical sizes of the order of 5 cm.

This might be the reason why in earlier studies a fast growth rate was reported. Such a high growth rate yields products that easily crack and the quality of these crystals is not good. Therefore, we lowered the low growth speed to 3 mm/h, while both feed and seed rods were counter-rotated at the rates of 20–40 rpm. Finally, we obtained boules with typically 5 cm length. The corresponding growth direction changed to [1 0 2] compared to the [0 0 1] direction in single crystals grown with faster growth rate. Our as-grown single crystals were oriented by Laue diffraction, and cut into different rectangular plates of 1 mm thickness and with edges parallel to the crystallographic principal axes.

The magnetic properties of our samples were studied using a SQUID magnetometer (MPMS-5XL, Quantum Design, Inc.). The measurements of specific heat were carried out using a standard thermal relaxation calorimetric method in a commercial Physical Property Measurement System (PPMS, Quantum Design Inc.).

Polarized neutron scattering experiments were performed at the IN12 triple-axis spectrometer at Institut Laue-Langevin and diffuse neutron scattering spectrometer DNS at the Heinz Maier-Leibnitz Zentrum. The measurements at IN12 have been carried out using CryoPad setup for spherical neutron polarimetry. The flipping ratio was 21. The measurements at DNS we have done with two different setups. In the standard setup for xyz-polarization analysis we have studied the scattering in spin-flip and non-spin-flip channels for three different neutron polarizations. In this case the magnetic field at the sample was limited to the instrument guide field (around 10 G). The flipping ratio was above 26. Additionally, we have measured the sample mounted between two permanent magnets providing the field the sample roughly around 2.5 kG. In this case due to the depolarization of the neutron beam by magnets, we performed no polarization analysis. The incoming wavelength for all measurements at DNS was $\lambda = 4.2$ Å.

Temperature dependent powder x-ray diffraction measurements have been performed on a powder x-ray diffractomter (Bruker D8 Discover A25) which is equipped with a Johansson monochromator for Cu-Kα radiation and which was optimized

for low background and high resolution. The measurements of our (crushed) single crystals confirm the absence of impurity phases. The temperature dependence of the lattice constants was measured using a He cryostat (Oxford Phenix).

For dielectric measurements, the plate-shaped samples were further polished thinner to a thickness of 0.1–0.3 mm. We applied silver paint to both sides as electrodes to form a parallel-plate capacitor. The samples were glued on the cryogenic stage of the customized probe that was inserted into a cryostat. A high-precision capacitance bridge (AH2700a, Andeen-Hagerling Inc.) or a LCR meter (E4980AL Keysight Technologies) was used for the dielectric measurements. The main sources of errors such as residual impedance in the whole circuit have been carefully compensated. In our measurements, various excitation levels (from 100 meV to 10 V) were used and no apparent difference was found, thus confirming the intrinsic nature of our observations.

To verify the ferroelectric nature of the possible multiferroic transitions, the spontaneous electric polarization (P) has been measured via the integration of the corresponding pyroelectric current. First, we fully polarized the specimens with a static electric field of 1000 kV/m during the cooling process from temperatures above T_N, then removed the electric field and short circuited the sample at lowest temperature in order to remove any possible trapped charge carriers. The pyroelectric current was, then, measured during the warming process at different heating rates (2–4 K/min).

III. EXPERIMENTAL RESULTS

A. Magnetic properties

We measured the temperature dependence of the magnetic susceptibility χ of a Bi_2CuO_4 single crystal in different magnetic fields and field directions (from 0.1 T to 5 T and with H parallel to c or a axis). In the zero-field-cooling (ZFC) and the field-cooling (FC) $\chi(T)$ curves no essential difference was observable.

As shown in Fig. 2(a), $\chi(T)$ increases on cooling, reaches its maximum within a broad hump around ~50 K, drops abruptly around ~43.5 K, and decreases further until an upturn below ~20 K occurs. The broad hump in $\chi(T)$ is indicative for short-range fluctuations. The drop around ~43.5 K indicates the emergence of long-range AFM order (i.e., T_N); see also $d\chi/dT(T)$ in the inset of Fig. 2(b) which exhibits a sharp peak at $T_N \sim 43.5$ K. A strong anisotropy of $\chi(T)$ can even be observed at high temperature. We plotted the temperature dependent inverse susceptibility (χ^{-1}) in Fig. 2(b). A strong deviation from linear behavior can be observed especially for $H \| a$ even at high temperatures above T_N. Apparently, a simple Curie-Weiss law is not applicable to Bi_2CuO_4. Note that also ESR experiments [17] report an anisotropic g factor for Bi_2CuO_4.

Whereas the susceptibility of Bi_2CuO_4 is field independent above T_N it exhibits an unusual field dependence below T_N (for $H \| a$)—up to ~1 T χ is increasing with increasing size of H. Moreover, we measured the field-dependent magnetization and susceptibility at different temperatures. As shown in Figs. 3(a) and 3(b) the M-H curve is nonlinear below 0.5–1 T for $H \| a$ and for temperatures below T_N. This behavior might

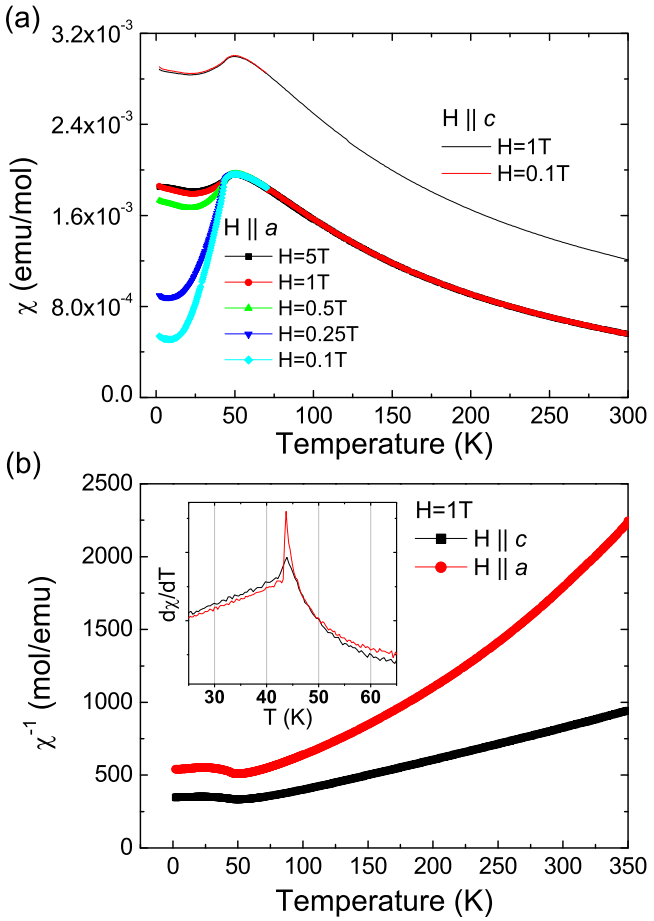

FIG. 2. (a) Temperature dependence of magnetic susceptibility, χ, measured for various magnitudes and directions of the magnetic field. (b) The corresponding temperature dependence of $1/\chi$. The derivative ($d\chi/dT$) is shown in the inset of panel (b).

be indicative of a metamagnetic transition with a kind of spin reorientation. In contrast to that we observe only linear M-H relations and field-independent susceptibilities for $H \perp a$. Our results for Bi_2CuO_4 are consistent with older studies in literature [11,20].

B. Polarized neutron scattering

To resolve the long-standing controversy regarding the orientation of ordered Cu spins [7,10–20], we studied the magnetic structure of Bi_2CuO_4 by polarized neutron diffraction. Figure 4 shows the magnetic neutron scattering intensities in the σ_{zz} and σ_{yy} spin-flip channels. No intensity in the σ_{yy} channel is observed. Hence the magnetic moments in Bi_2CuO_4 have no projection on the c axis and are entirely aligned within the ab plane. Thus the c-axis alignment of the copper spins as suggested in Refs. [7,10] can be discarded and the alignment within the ab plane [11] is corroborated. We obtained the same result in a polarized neutron measurement at 3.5 K using the DNS spectrometer at the FRM II; see Fig. 5.

The magnetoelectrically induced ferroelectricity in Bi_2CuO_4 discussed in Sec. III G prompted us to look for signs of an incommensurate spin ordering in this material. Many frustrated magnets showing an incommensurate spiral

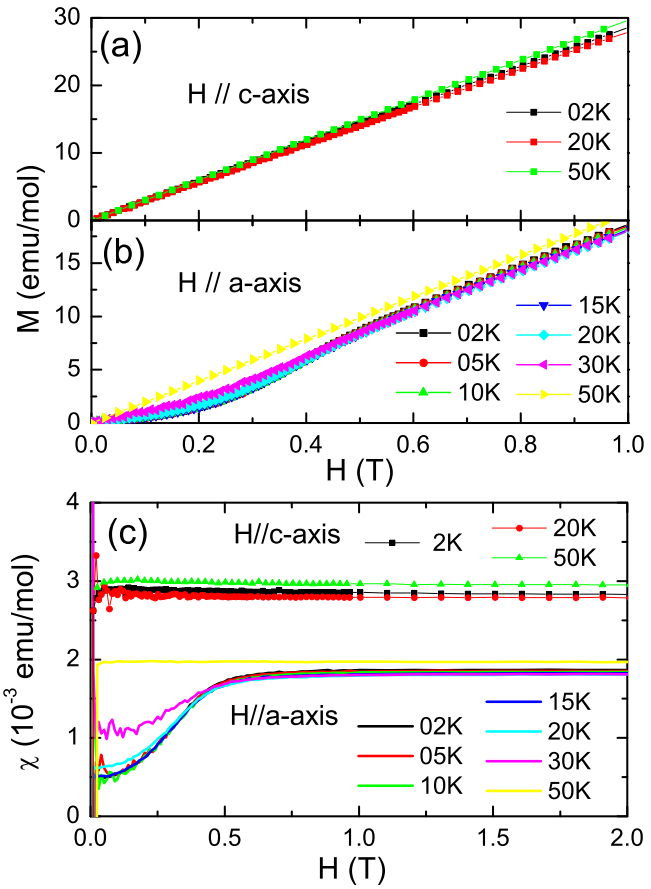

FIG. 3. Field dependence of magnetization and magnetic susceptibility with external magnetic field applied along the c and a axes.

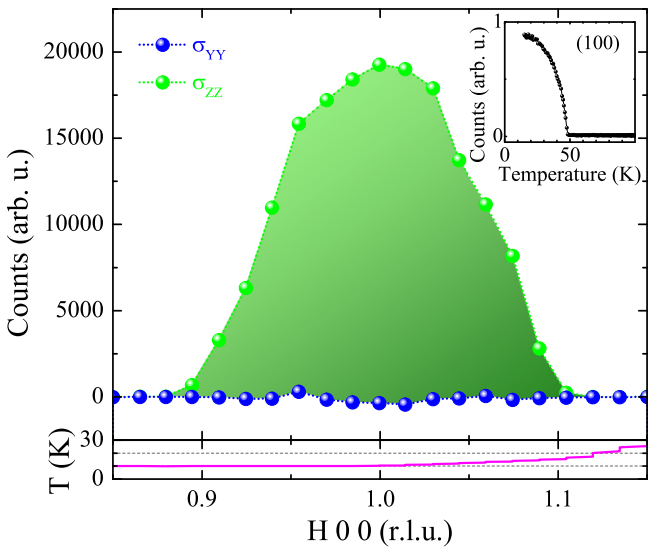

FIG. 4. Polarization dependence of the magnetic (100) reflection measured at the IN12 spectrometer. The green and blue data points denote the magnetic neutron scattering intensities in the σ_{zz} and σ_{yy} spin-flip channels with the x axis being parallel to the scattering vector and z axis being perpendicular to the scattering plane. The lower figure shows the sample temperature at each measuring point of that scan which is always well below T_N. The temperature dependence of the magnetic (100) reflection is shown in the inset.

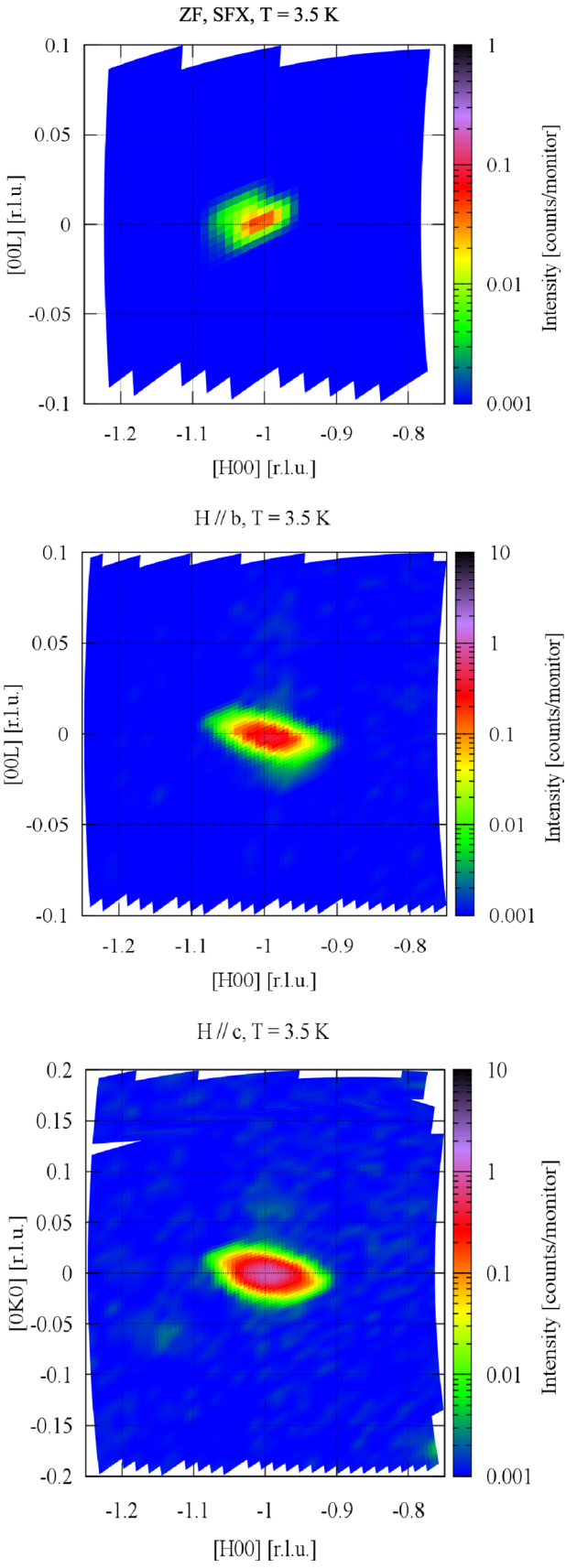

FIG. 5. Intensity of the magnetic (100) reflection measured at the DNS spectrometer in zero field (upper plot) and in the magnetic fields H of about 2.5 kG.

ordering are ferroelectric and competing exchange interactions in Bi_2CuO_4 can lead to an instability of a uniform antiferromagnetic state. In fields up to ~0.25 T we could not observe any incommensurability within the experimental resolution of our measurements at the DNS spectrometer (see Fig. 5). Further high-resolution experiments in higher magnetic fields would be desirable.

C. Lattice parameters

We have measured Bi_2CuO_4 by means of powder x-ray diffraction on a powder x-ray diffractometer (Cu-Kα radiation) that we optimized for high resolution. Within these measurements we were not able to find any indications for the occurrence of peak splittings or superstructure reflections below 300 K. However, our high resolution measurements are able to resolve an anomalous increase of the a- and an anomalous decrease of the c-lattice constant on cooling through T_N, see Fig. 6. This is indicative for magneto elastic coupling as was also observed in other transition metal compounds [42,43]. Our observed anomalous increase of the lattice constants is in agreement with reported thermal expansion measurements [16].

D. Heat capacity

Further evidence for long-range antiferromagnetic order in Bi_2CuO_4 is revealed from our specific heat (C_p) measurements. As shown in Fig. 7, $C_p(T)$ shows a λ-shaped anomaly at T_N. We have measured the specific heat also on heating and on cooling around T_N; see the upper left inset of Fig. 7. The absence of any hysteresis indicates a second order phase transition. This is also consistent with the absence of any structural transition at T_N observed in our powder x-ray diffraction measurements.

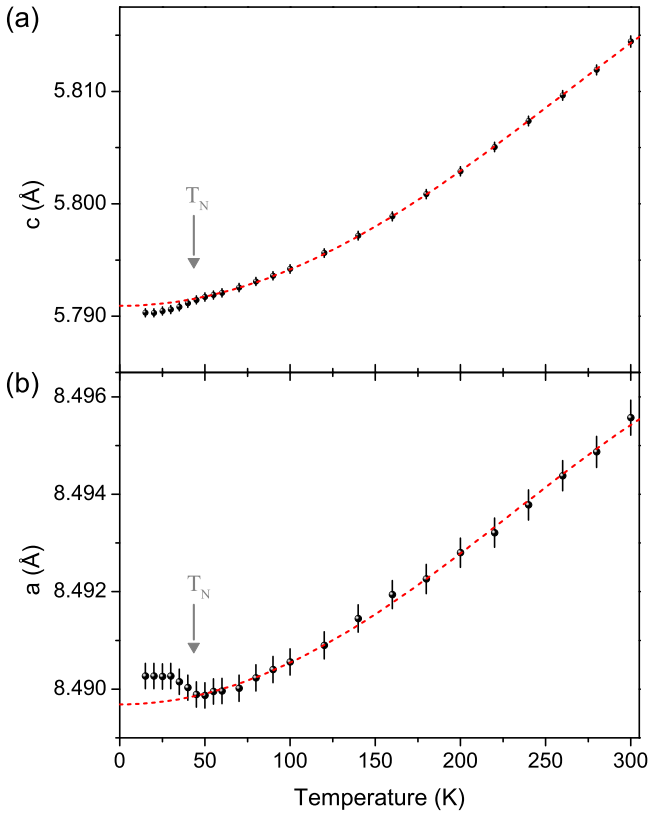

FIG. 6. Temperature dependence of the lattice parameters. The red dashed line indicates a fit to the data above T_N. Below T_N an anomalous increase (decrease) of the a (c) lattice constant is observable. This observation is in agreement with high-resolution thermal expansion measurements.

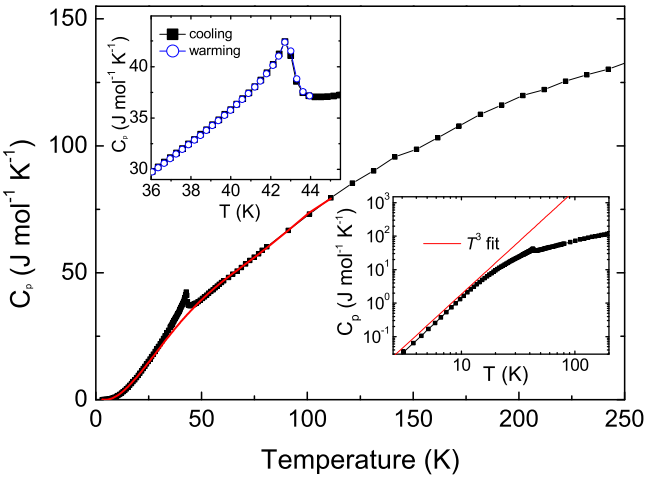

FIG. 7. Temperature dependence of the specific heat, $C_p(T)$, for Bi_2CuO_4 single crystal. The red line represents the background to be subtracted to estimate the change in entropy from the anomaly peak around T_N. The upper right inset focuses on $C_p(T)$ in the region around the magnetic transition, and two sets of C_p data are shown, measured during warming (solid square) and cooling processes (open circles), respectively. The $C_p(T)$ is also plotted on the log-log scale in the bottom right inset, with a T^3 (Debye) fit (red line) to the low temperature part of $C_p(T)$.

Both lattice vibrations (phonons) and magnetic excitations (magnons) contribute to the specific heat C_p. At low temperatures the phonon contribution of C_p obeys the Debye T^3 power law. As can be seen in the lower right inset in Fig. 7, the low temperature part of $C_p(T)$ can be fitted quite well with a function proportional to T^3, thus suggesting that also the magnetic contribution of C_p obeys a T^3 law. The T^3 dependence—rather than $T^{3/2}$ behavior—further confirms long-range AFM ordering in Bi_2CuO_4. However, it remains difficult to extract the pure magnetic part of $C_p(T)$ accurately due to the absence of nonmagnetic isostructural materials in order to estimate the contribution of the lattice vibrations to the total specific heat. To get a rough estimate of the entropy removed by the magnetic ordering, which is remarkably indicated by the peak of $C_p(T)$ around T_N, we use a polynomial fit to the high-temperature (>60 K) and low-temperature (<25 K) regimes for the background (the red solid line shown in main panel of Fig. 7). The entropy obtained from integrating the peak in $C_p(T)/T$ (for 25 K < T < 60 K) amounts to 1.82 J mol^{-1} K^{-1} which is only 32% of the full magnetic entropy associated with $R \cdot \ln(2S+1) \approx 5.76$ J mol^{-1} K^{-1} as expected for an $S = 1/2$ spin system.

E. Anisotropic dielectric properties as zero field

In view of the tetragonal symmetry of Bi_2CuO_4 we measured the dielectric constant for an electric field E applied

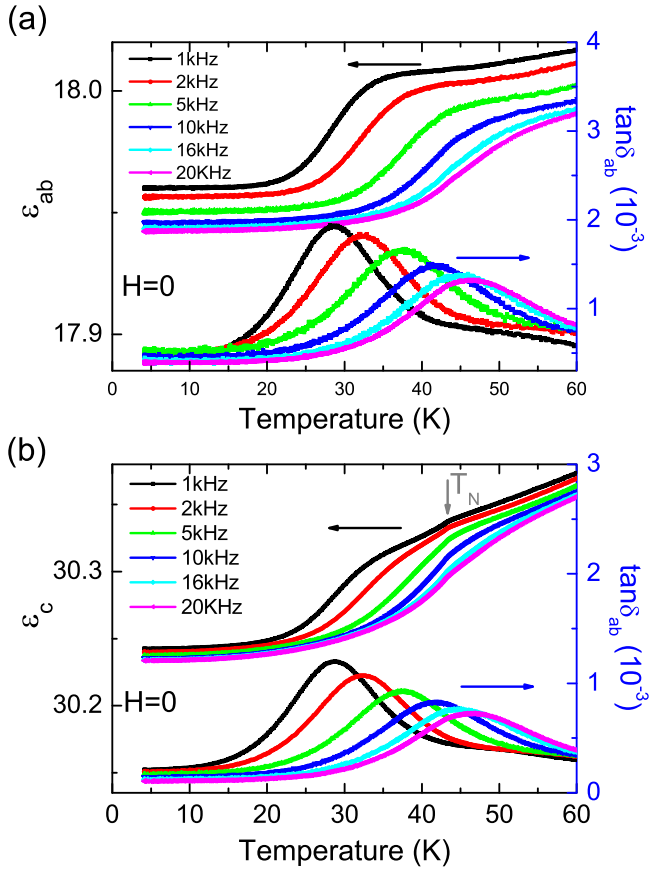

FIG. 8. Temperature dependence of dielectric contants: (a) ε_{ab} ($E \perp c$ axis) and (b) ε_c ($E \| c$ axis). Also shown is the corresponding dielectric loss (tanδ). All data has been measured in zero field (H=0). The vertical arrow in (b) marks T_N where the slight kink occurs.

either within the ab plane, ε_{ab}, or along the c axis, ε_c. Two thin plate samples that were cut from our floating-zone-grown single crystal were used to investigate the anisotropic dielectric properties.

Figure 8 shows the temperature-dependent ε_c and ε_{ab} measured in zero field for different frequencies. We observed an anisotropy in permittivity: $\varepsilon_{ab} \sim 18$ is distinctly lower than $\varepsilon_c \sim 30$, which resembles the anisotropy in magnetic susceptibility discussed above.

Both ε_c and ε_{ab} slightly decrease with decreasing temperature and saturate at lowest temperature. ε_{ab} and ε_c also exhibit a strong frequency dependence characteristic of a Debye-type dipolar relaxationlike behavior. For analysis of the frequency dispersion, the corresponding dielectric loss (tanδ) curves are also shown. At each measuring frequency the loss exhibits a peak corresponding to the kneelike change of ε. As frequency increases, the peak shifts to higher temperatures with a concomitant decrease of magnitude. The peak temperature and the frequency can be fitted with the Arrhenius law, $f = f_0 \exp(-Q/kT_{\text{peak}})$, where f is the characteristic frequency, k is the Boltzmann constant, T_{peak} is the peak temperature, f_0 is a prefactor, and Q is the activation energy. Fitting the two sets of data from Figs. 8(a) and 8(b) yields nearly the same activation energy of ~22 meV.

Across the magnetic ordering temperature T_N, a weak "kink" appears in $\varepsilon_c(T)$ at all frequencies. However, no corresponding anomalous behavior was found in the dielectric loss indicating the absence of ferroelectric transition in zero field. This conclusion is corroborated by our pyroelectric measurements discussed below. No anomaly is observed in $\varepsilon_{ab}(T)$.

F. In-plane dielectric response in an applied magnetic field

Next we studied the in-plane dielectric properties under applied magnetic fields. We present the data measured at 1 kHz because of the relatively large separation of the dispersion peak from T_N and a better signal-to-noise ratio at low frequencies.

We applied H parallel and perpendicular to the measuring electric field E. Up to 9 T no change can be observed in ε_{ab} and tanδ_{ab}, as shown in Fig. 9. The corresponding pyroelectric

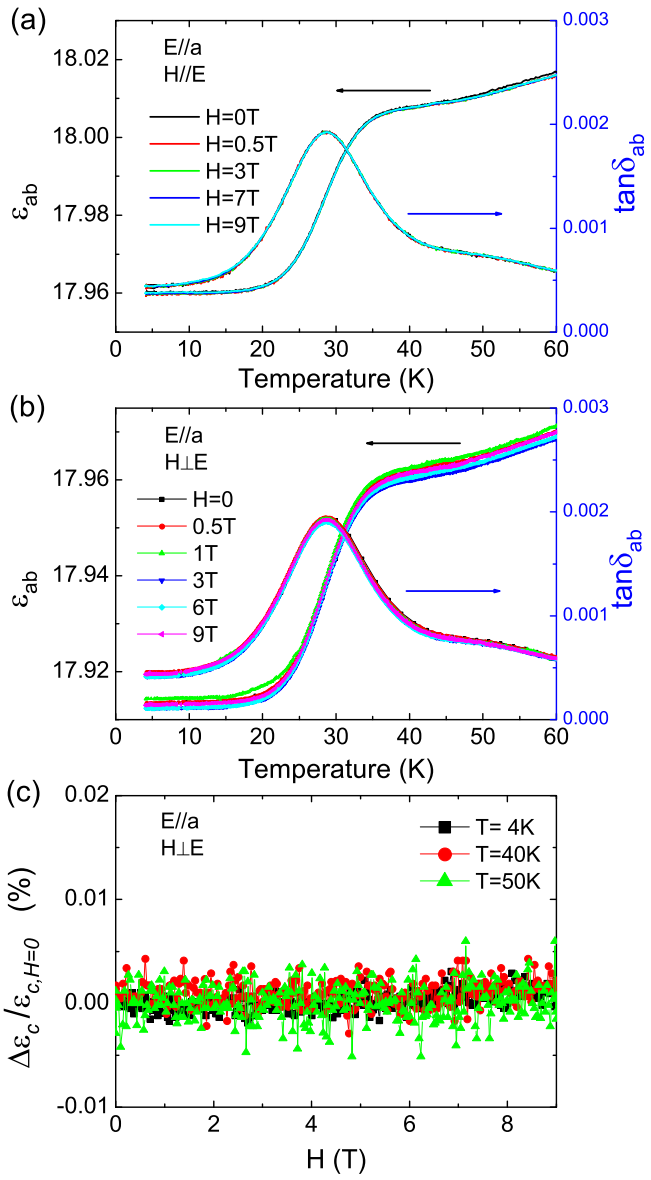

FIG. 9. Temperature dependence of in-plane dielectric constants ε_{ab} and corresponding loss for (a) $H \| E$ and (b) $H \perp E$. The corresponding dielectric loss (tanδ) is also shown. The measurement frequency amounts to 1 kHz. (c) The magnetic field induced change of the dielectric constant (measured at 1 kHz) at different temperatures (4 K, 40 K, and 50 K).

measurements also show no electric polarization (not shown). We also investigated the in-plane magnetodielectric effect at temperatures below and above T_N for several values of the applied field H. As shown in Fig. 9(c) for $H \perp E$ no magnetodielectric effect is observed. Similar results were found for $H \parallel E$.

G. Out-of-plane dielectric properties in an applied field and magnetically induced ferroelectricity

In this section we describe the effect of magnetic field on the dielectric permitivity along the tetragonal c axis, ε_c. We show that under an applied magnetic field Bi_2CuO_4 becomes ferroelectric with the field-dependent electric polarization, P_c, parallel to the c axis.

1. Out-of-plane dielectric response in $H \parallel c$

We performed dielectric measurements for a variety of magnetic fields applied along the c direction. Figure 10 shows the detailed results for $H = 9$ T. The most remarkable observation is the sharp λ-shaped peak observed in both $\varepsilon_c(T)$ and $\tan\delta_c$ for all frequencies, which is indicative of a ferroelectric transition. The peak position is independent of frequency and coincides with T_N determined from magnetic susceptibility and specific heat measurements. Compared with the zero field data Fig. 8(b) shows that the frequency-dependent dielectric relaxation behavior is essentially unaffected by the external magnetic field.

The direct evidence for the ferroelectric nature of the transition at T_N is given by our pyroelectric current measurements shown in Fig. 10(c). A small but very sharp peak emerges as temperature approaches T_N. The pyroelectric current drops to zero above T_N. The corresponding c-axis electric polarization, P_c, obtained by integrating the pyroelectric current, appears below T_N and reaches its (rather small) saturation value of about 0.32 $\mu C/m^2$. The reversal of the poling electric field changes sign of P_c. This proves the emergence of ferroelectricity in Bi_2CuO_4under the applied magnetic field.

Figure 11 shows $\varepsilon_c(T)$ measured at the frequency 1 kHz for different applied magnetic fields ranging from 0 to 9 T. The small kink around T_N observed in zero field remains unchanged for magnetic fields up tp ∼0.5 T. As the magnetic field is increased further, a dielectric peak appears [see, e.g., the blue curve measured at 1.5 T in the inset of Fig. 11(a)]. This dielectric peak develops gradually with increasing H and no saturation is observed up to our instrumental limit of 9 T. The transition temperature T_N at which the peak is observed is almost unaffected by H. The same behavior is observed in the corresponding loss curves shown in Fig. 11(b). Hence the dielectric anomaly associated with the onset of ferroelectricity in Bi_2CuO_4 appears for applied magnetic fields (>∼0.5 T) and becomes more pronounced as the magnetic field increases. The results for field and temperature dependence of P_c [Fig. 11(c)] clearly show that Bi_2CuO_4 becomes ferroelectric under an applied magnetic field $H \| c$.

We also studied the magnetodielectric coupling for $H \| c$, i.e., the dependence of the dielectric constant on an applied magnetic field. Figure 11(d) shows the relative change of the permittivity, $\frac{\Delta\varepsilon}{\varepsilon} = \frac{\varepsilon_c(H)-\varepsilon_c(0)}{\varepsilon_c(0)}$, for several temperatures below and above the transition temperature, T_N. A prominent

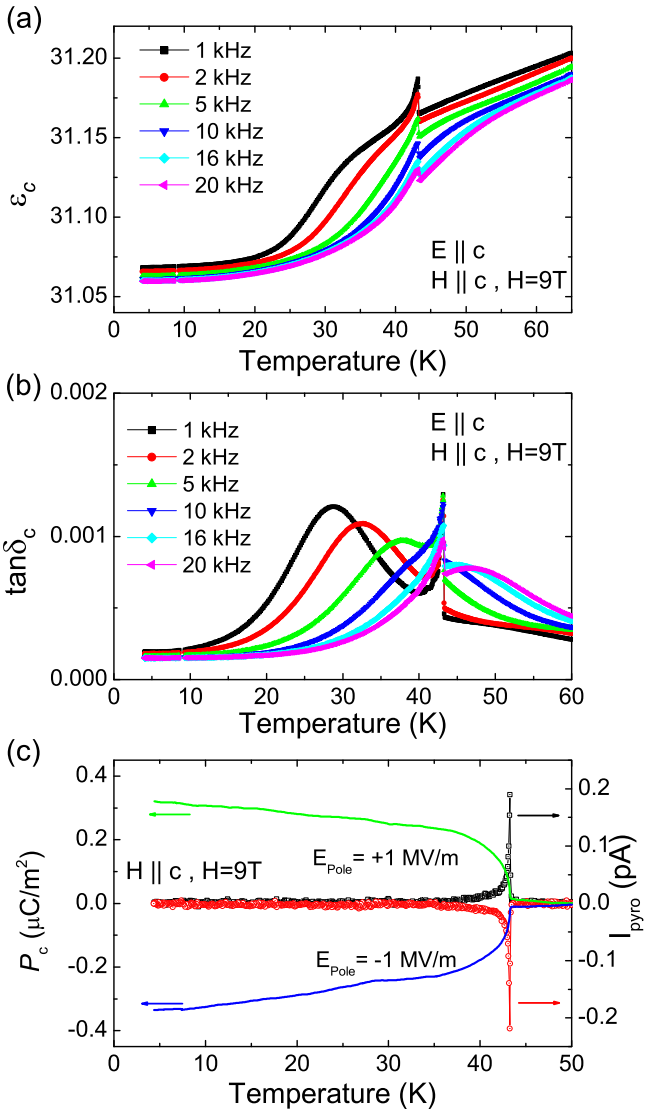

FIG. 10. Temperature dependence of (a) the c-axis dielectric constant ε_c and (b) the tan loss for different frequencies measured in a field of $H = 9$ T along the c axis. (c) The pyroelectric currents (black and red dots) measured with both positive and negative poling electric fields of 1 MV/m applied. The corresponding polarization (P_c, green and blue solid lines) obtained by integrating the pyroelectric currents from above T_N.

magnetodielectric effect is only observed for T close to T_N. At $T = 43$ K, the value of $\frac{\Delta\varepsilon}{\varepsilon}$ grows with increasing field H (>1 T) reaching ∼0.06% at 9 T.

2. Out-of-plane dielectric response in $H \parallel a$

We performed similar measurements for magnetic fields applied along the a direction ($H \perp E$). The results are shown in Fig. 12. In contrast to the behavior observed for $H \| c$, the dielectric peak in $\varepsilon_c(T)$ at T_N is discernible already at very low magnetic fields. At about ∼0.5 T the peak reaches its maximum size and becomes smaller as H is increased further [see the inset in Fig. 12(a)]. Concomitantly with the peak in ε_c, a sharp peak in the dielectric loss, tan δ_c, appears and disappears [see Fig. 12(b)].

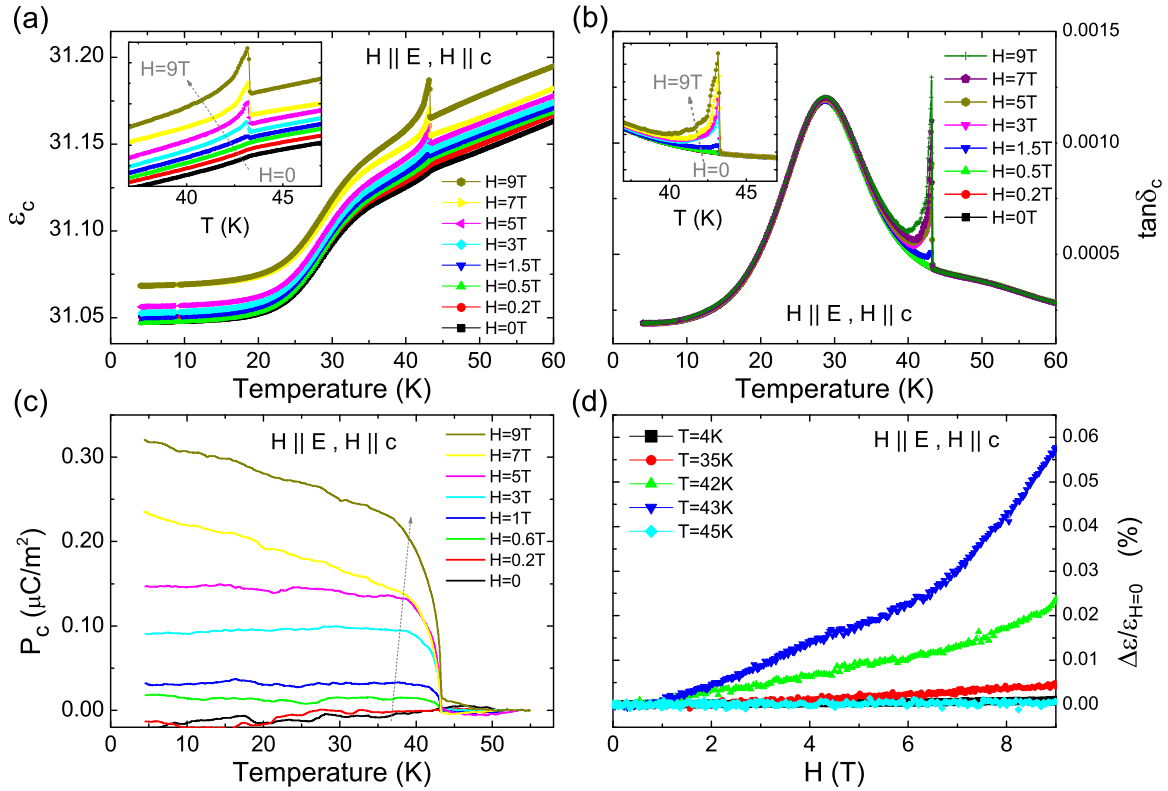

FIG. 11. Temperature dependence of (a) ε_c, (b) tan loss, and (c) polarization measured in different fields along the c axis. (d) The magnetic field induced change of ε_c at different temperatures (from 4 K to 45 K). The measuring frequency amounts to 1 kHz.

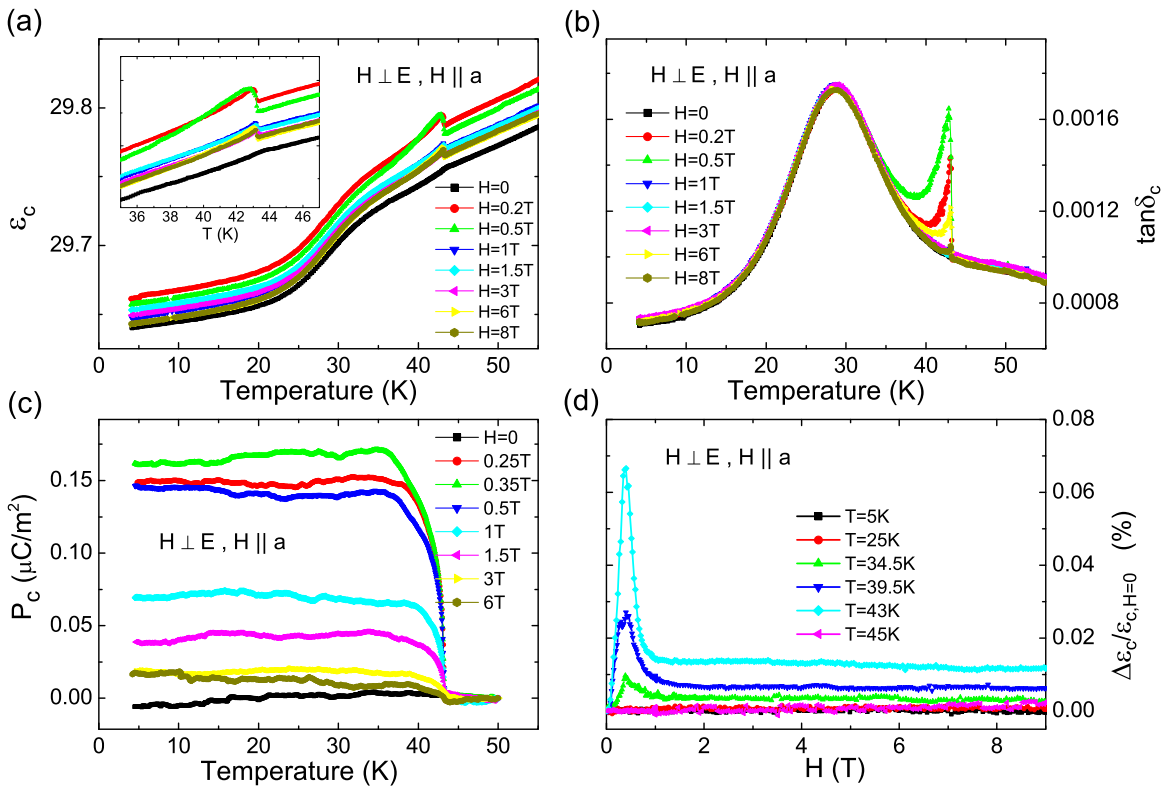

FIG. 12. Temperature dependence of (a) ε_c, (b) tan loss, and (c) the polarization measured in different magnetic fields applied along the a direction. (d) The magnetic field induced change in ε_c at different temperatures (from 5 K to 45 K). The measuring frequency is 1 kHz.

Figure 12(c) shows the electric polarization P_c measured in $H\|a$. A low field of just 0.2 T induces ferroelectricity in Bi_2CuO_4 with a spontaneous polarization of about 0.14 $\mu C/m^2$ at 4 K. After P_c reaches its maximum value, it decreases upon further increase of the magnetic field and vanishes around 6 T.

Finally, we also studied the magnetodielectric effect for $H\|a$. As for $H\|c$, there is no discernible magnetodielectric effect at temperatures far from T_N. Only around the dielectric peak region we are able to observe a prominent magnetodielectric effect in low fields. At 43 K, $\frac{\Delta\varepsilon}{\varepsilon}$ rises sharply with increasing field up to its maximum value at about ~0.5 T, and then decreases upon further increase of H.

IV. DISCUSSION

In zero field, previous neutron diffraction measurements on Bi_2CuO_4 reveal a $k = 0$ collinear spin structure with parallel spins in the chains running along the c and antiparallel spins in neighboring chains. However, the orientation of ordered magnetic moments is poorly understood and remains controversial. In other magnetic Cu^{2+} ($S = 1/2$) compounds with the CuL_4 (L = O, Cl, Br) square-planar coordination (e.g., in $CuCl_2 \cdot 2H_2O$, $CuCl_2$, $CuBr_2$, or $LiCuVO_4$) an easy-plane anisotropy is observed. Our polarized neutron data suggest that this is also the case for Bi_2CuO_4.

Our observation of a metamagnetic behavior in low in-plane fields (of about ~0.5 T at 2 K) is consistent with previous findings [11,20]. The nonlinearity of the $M(H)$ curve likely originates from the field-dependent volume fraction of the four antiferromagnetic domains, in which spins are (anti)parallel to the a or b axis. We cannot exclude, however, a more complex spin-reorientation transition taking place at $H_a \sim 0.5$ T.

Concomitant with the emergence of a long range magnetic ordering at T_N, we observe a transition into a ferroelectric state with the polarization along the c direction, which appears under an applied magnetic field. This transition is manifest in both the dielectric constant, $\varepsilon_c(T,H)$, and polarization, $P_c(T,H)$, measurements. The transition occurs for magnetic fields applied either in the ab plane or along the c direction. The electric polarization P_c as a function of the magnetic field along the a and c axes at 35 K (at which the polarization nearly saturates) is shown in Fig. 13. As we discuss below, the magnetoelectric response provides important additional information on magnetic ordering in Bi_2CuO_4.

Although the magnetic field dependence of the electric polarization is nonlinear, the most likely source of the field-induced ferroelectricity is the linear magnetoelectric effect [32–34]. We assume that the antiferromagnetic order parameter in Bi_2CuO_4 is $\mathbf{L} = \mathbf{M}_1 - \mathbf{M}_2 + \mathbf{M}_3 - \mathbf{M}_4$, where $\mathbf{M}_i$ ($i = 1,2,3,4$) is the sublattice magnetization labeled by the four independent Cu sites occupying the $4c$ Wykoff positions in the crystallographic unit cell with the coordinates $\mathbf{r}_1 = (1/4,1/4,z)$, $\mathbf{r}_2 = (3/4,3/4,1/2 - z)$, $\mathbf{r}_3 = (1/4,1/4, 1/2 + z)$, and $\mathbf{r}_4 = (3/4,3/4, -z)$. Spatial inversion, $\mathbf{r} \to -\mathbf{r}$, interchanges the sites 1 and 4 and the sites 2 and 3, so that under inversion $\mathbf{L}$ changes sign. The inversion symmetry breaking by this antiferromagnetic ordering allows for a linear magnetoelectric effect. We note that the noncentrosymmetric antiferromagnetic order is incompatible with the interpretation

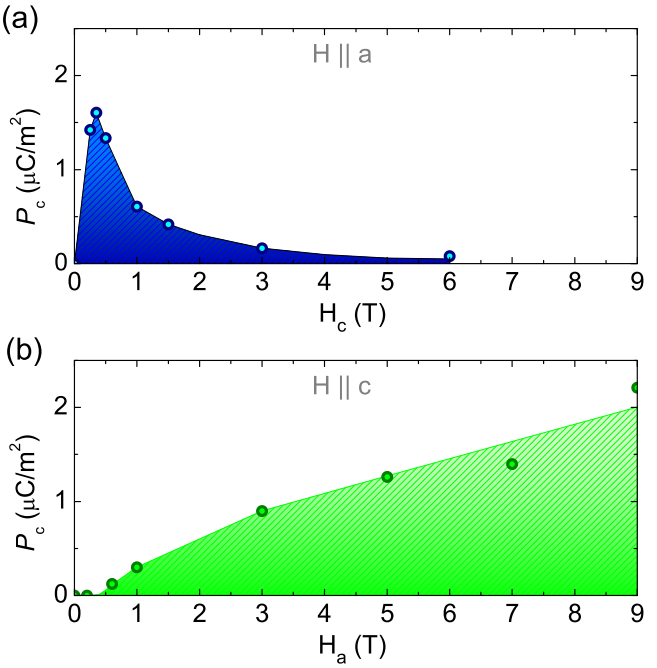

FIG. 13. Phase diagram of Bi_2CuO_4 at 35 K which contains the information about the magnetic field dependence of the electric polarization P_c for two different field directions: (a) $H\|a$ and (b) $H\|c$.

of the metamagnetic behavior in terms of a weak ferromagnetic moment [44].

The free energy density describing the linear magnetoelectric coupling contains four terms allowed by *P4/ncc* symmetry of the crystal lattice,

$$f_{\rm me} = -g_1(L_aH_a + L_bH_b)E_c - g_2(H_aE_a + H_bE_b)L_c - g_3(E_aL_a + E_bL_b)H_c - g_4L_cH_cE_c, \quad (1)$$

where g_α ($\alpha = 1,2,3,4$) are the coupling constants. The c component of the electric polarization induced by an applied magnetic field is then

$$P_c = -\partial f_{\rm me}/\partial E_c = g_1(L_aH_a + L_bH_b) + g_4L_cH_c. \quad (2)$$

Similar expressions can be obtained for P_a and P_b, but since no significant in-plane electric polarization was observed, the coupling constants g_2 and g_3 must be relatively small.

We first discuss the magnetoelectric behavior of Bi_2CuO_4 in $H\|a$ [see Figs. 12(c) and 13(a)]. Our polarized neutron scattering data show that in zero field the antiferromagnetic vector $\mathbf{L}$ lies in the ab plane. It can be oriented either along the crystallographic axes (the $\pm[100]$ and $\pm[010]$ directions) or along the diagonals (the $\pm[110]$ and $\pm[1\bar{1}0]$ directions). In the latter case, the magnetic field parallel to the a axis would result in a gradual rotation of $\mathbf{L}$ toward the [100] plane. Instead, we observe a metamagnetic transition at $H_a \sim 0.5$ T (see Fig. 3), which indicates that in zero field Bi_2CuO_4 is divided into domains with $L\|a$ and $L\|b$. The zero-field magnetic susceptibility is then the average of the longitudinal ($L \parallel H$) and transverse ($L \perp H$) magnetic susceptibilities. Above the metamagnetic transition the L_a domains disappear and the magnetic susceptibility becomes purely transversal,

which explains why above ∼0.5 T it increases approximately by factor of 2 (see Fig. 3). The peculiar dependence of P_c on H_a shown in Fig. 13(a) is consistent with this scenario. As follows from Eq. (2), the linear magnetoelectric coefficient $\alpha_{ca} = \frac{\partial P_c}{\partial H_a} = g_1 L_a$, which is why P_c grows linearly with the field below ∼0.5 T, when the L_a domains are present, and decreases above ∼0.5 T, when these domains disappear.

Below we discuss the spin-reorientation transition in more detail. Because of tetragonal symmetry of Bi_2CuO_4, the $L\|b$ state has a lower free energy than the $L\|a$ for an arbitrarily small H_a. However, in low applied magnetic fields the motion of domain walls separating the $L\|a$ and $L\|b$ domains can be hindered by pinning and the ferroelectric state with $L_a \neq 0$ can survive as a metastable state. There is, however, an upper critical field, H_{cr}, above which the ferroelectric state becomes locally unstable and disappears. This can explain the nature of the metamagnetic transition observed at ∼0.5 T.

This transition as well as the observed magnetoelectric response can be described using the phenomenological Landau theory. Assuming that both the vector order parameter and the applied magnetic field are confined to the ab plane, while the electric field is parallel to the c axis, we can write the free energy density of Bi_2CuO_4 in the form

$$f \approx \frac{a}{2}L^2 + \frac{b_1}{4}L^4 + \frac{b_2}{2}L_a^2 L_b^2 + \frac{c_1}{2}L^2H^2 + \frac{c_2}{2}(\mathbf{L}\cdot\mathbf{H})^2 + c_3 L_a L_b H_a H_b - \frac{\chi_0}{2}H^2 - g_1(\mathbf{L}\cdot\mathbf{H})E_c, \quad (3)$$

where $L^2 = L_a^2 + L_b^2$, $H^2 = H_a^2 + H_b^2$, $(\mathbf{L}\cdot\mathbf{H}) = L_a H_a + L_b H_b$, χ_0 is the background magnetic susceptibilty, and $a = \alpha(T - T_N(0))$, $T_N(0)$ being the transition temperature in zero magnetic field. The quartic anisotropy coefficient, $b_2 > 0$, favors $\mathbf{L}$ (anti)parallel to the a and b axes, while $c_2 > 0$ favors $\mathbf{L} \perp \mathbf{H}$.

Minimizing the free energy Eq. (3) with respect to L_a for $L_b = H_b = 0$, we obtain the order parameter in the metastable state,

$$L_a^2 = \frac{\alpha(T_N(H_a) - T)}{b_1}, \quad (4)$$

where $T_N(H_a) = T_N(0) - \frac{(c_1+c_2)}{\alpha}H_a^2$ is the transition temperature in the applied field. The (temperature-dependent) critical field, H_{cr}, above which this state is unstable, is given by

$$H_{cr}^2 = \frac{\alpha(T_N(0) - T)b_2}{b_1 c_2 + b_2(c_1 + c_2)}. \quad (5)$$

The electric polarization, given by Eq. (2), is approximately proportional to H_a, for $H_a < H_{cr}$ (the magnetic field dependence of L_a [see Eq. (4)] is weak, since our experiment shows that the transition temperature is practically field independent). Finally, the dielectric susceptibility associated with the antiferromagnetic order is given by

$$\chi_c = \left.\frac{\partial P_c}{\partial E_c}\right|_{E_c=0} = \chi_L g_1^2 H_a^2, \quad (6)$$

where χ_L is the antiferromagnetic susceptibility: $\chi_L = (\frac{\partial^2 f}{\partial L_a^2})^{-1} \propto |T - T_N(H_a)|^{-1}$ near the transition (see Ref. [45], where also the effect of spin fluctuations on the critical behavior of the dielectric susceptibility of a linear magnetoelectric material is discussed). The dielectric susceptibility diverges because in the applied magnetic field a linear magnetoelectric material becomes ferroelectric, since for $H_a \neq 0$ the antiferromagnetic order, L_a, is linearly coupled to the electric field, E_c. Equation (6) is consistent with our observations (see Sec. III G 2): the magnetic field dependence of ε_c is only strong close to T_N, where the divergence of χ_c compensates for the weakness of the magnetoelectric response.

The explanation of the magnetoelectric response in $H\|c$ [see Figs. 11(c) and 13(b)] is less straightforward. According to Eq. (2), the linear magnetoelectric coefficient $\alpha_{cc} = \frac{\partial P_c}{\partial H_c} = g_4 L_c$ is only nonzero if $L_c \neq 0$. However, L_c is zero in zero field and $H\|c$ is unlikely to result in a transition that rotates $\mathbf{L}$ out of the ab plane. Also the linear dependence of M_c on H_c [Figs. 3(a) and 3(c)] shows the absence of any transition. One possible explanation is a small in-plane magnetic field component resulting from a small misalignment of the sample or demagnetizing fields. Note that α_{cc} is ∼15 times smaller than α_{ca} for $H_a < 0.5$ T.

Another possible explanation is that the actual symmetry of Bi_2CuO_4 is lower than tetragonal. We did not, however, find any indication for a symmetry lowering, even though our high-resolution powder x-ray diffraction measurements allow us to resolve tiny thermal expansion effects (see Fig. 6). Ferroelectricity in Bi_2CuO_4 can, in principle, be induced by a complex magnetic ordering, such as an incommensurate spin spiral with a small wave vector. The rotation of the spiral plane in an applied magnetic field, which transforms a nonferroelectric helical spiral into a ferroelectric cycloidal spiral, can mimic linear magnetoelectric response, as was observed in the $CoCr_2Se_4$ spinel [46,47]. However, also in the spiral state scenario it is difficult to explain why the out-of-plane electric polarization is induced by both in-plane and out-of-plane magnetic fields.

V. CONCLUSIONS

A combination of several experimental techniques was applied to clarify the nature of magnetic ordering in floating zone grown Bi_2CuO_4 single crystals. Polarized neutron scattering measurements clearly show that ordered magnetic moments of Cu ions are confined to the ab plane, which resolves the long standing controversy. In addition, we observe a ferroelectric polarization parallel to the c axis induced by applied magnetic fields, which is consistent with inversion symmetry breaking by the C-type antiferromagnetic ordering. We argue that the electric polarization in the magnetic field parallel to the a axis originates from the linear magnetoelectric effect in a metastable state, which disappears above a critical magnetic field. The relatively weak response observed in the magnetic field parallel to the c axis does not seem to be compatible with symmetry of Bi_2CuO_4 and remains a puzzle. Further studies of the magnetic states of this material are necessary.

ACKNOWLEDGMENTS

The authors would like to thank L. H. Tjeng and O. Stockert for fruitful discussions and Ch. Becker, T. Mende, and S. Wirth for their support on the experimental construction of the dielectric measurement system.

[1] J. G. Bednorz and K. A. Müller, Z. Phys. B **64**, 189 (1986).
[2] J. C. Boivin, D. Tomas, and S. Tridot, C. R. Acad. Sci. C **276**, 1105 (1973).
[3] T. Masuda, A. Zheludev, A. Bush, M. Markina, and A. Vasiliev, Phys. Rev. Lett. **92**, 177201 (2004); **94**, 039706 (2005).
[4] P. Abbamonte, G. Blumberg, A. Rusydi, A. Gozar, P. G. Evans, T. Siegrist, L. Venema, H. Eisaki, E. D. Isaacs, and G. A. Sawatzky, Nature (London) **431**, 1078 (2004).
[5] D. F. Khozeev, A. A. Gippius, E. N. Morozova, A. N. Vasil'ev, A. V. Zalessky, W. Hoffmann, K. Luders, G. Dhalenne, and A. Revcolevshi, Physica B (Amsterdam) **284-288**, 1377 (2000).
[6] K. Sreedhar, P. Ganguly, and S. Ramasesha, J. Phys. C **21**, 1129 (1988).
[7] J. L. Garcia-Mufioz, J. Rodriguez-Carvajal, F. Sapina, M. J. Sanchis, R. Ibanez, and D. Beltran-Porter, J. Phys.: Condens. Matter **2**, 2205 (1990).
[8] R. Troc, J. Janicki, I. Filatow, P. Fischer, and A. Murasik, J. Phys.: Condens. Matter **2**, 6989 (1990).
[9] E. W. Ong, G. H. Kwei, R. A. Robinson, B. L. Ramakrishna, and R. B. Von Dreele, Phys. Rev. B **42**, 4255 (1990).
[10] J. Konstantinovic, G. Stanisic, M. Ain, and G. Parette, J. Phys.: Condens. Matter **3**, 381 (1991).
[11] K. Yamada, K. Takada, S. Hosoya, Y. Watanabe, Y. Endoh, N. Tomonaga, and T. Suzuki, J. Phys. Soc. Jpn. **60**, 2406 (1991).
[12] M. J. Konstantinovi, Z. V. Popovi, S. D. Devi, A. Revcolevschi, and G. Dhalenne, J. Phys.: Condens. Matter **4**, 7913 (1992).
[13] Z. V. Popovi, G. Kliche, M. J. Konstantinovi, and A. Revcolevschi, J. Phys.: Condens. Matter **4**, 10085 (1992).
[14] M. J. Konstantinovic and Z. V. Popovic, J. Phys.: Condens. Matter **6**, 10357 (1994).
[15] M. J. Konstantinović, Z. Konstantinović, and Z. V. Popović, Phys. Rev. B **54**, 68 (1996).
[16] B. D. White, W. M. Pätzold, and J. J. Neumeier, Phys. Rev. B **82**, 094439 (2010).
[17] H. Ohta, K. Yoshida, T. Matsuya, T. Nanba, M. Motokawa, S. Hosoya, K. Yamada, and Y. Endoh, J. Phys. Soc. Jpn. **61**, 2921 (1992).
[18] A. I. Pankrats, G. A. Petrakovskii, and K. A. Sablina, Solid State Commun. **91**, 121 (1994).
[19] H. Ohta, Y. I. S. Kimura, S. Okubo, H. Nojiri, M. Motokawa, S. Hosoya, K. Yamada, and Y. Endoh, Physica B (Amsterdam) **246**, 557 (1998).
[20] M. Herak, M. Miljak, G. Dhalenne, and A. Revcolevschi, J. Phys.: Condens. Matter **22**, 026006 (2010).
[21] O. Janson, R. O. Kuzian, S.-L. Drechsler, and H. Rosner, Phys. Rev. B **76**, 115119 (2007).
[22] S. Matsushima, K. Yamada, H. Nakamura, M. Arai, and K. Kobayashi, J. Ceram. Soc. Jpn. **116**, 589 (2008).
[23] G. A. Petrakovskii, K. A. Sablina, V. V. Valkov, B. V. Fedoseev, A. Furrer, P. Fischer, and B. Roessli, JETP Lett. **56**, 144 (1992).
[24] M. Aïn, G. Dhalenne, O. Guiselin, B. Hennion, and A. Revcolevschi, Phys. Rev. B **47**, 8167 (1993).
[25] A. Goldoni, U. del Pennino, F. Parmigiani, L. Sangaletti, and A. Revcolevschi, Phys. Rev. B **50**, 10435 (1994).
[26] A. Ghosh and S. Hazra, Solid State Commun. **106**, 677 (1998).
[27] K. Yoshii, T. Fukuda, H. Akahama, J. Kano, T. Kambe, and N. Ikeda, Physica C (Amsterdam) **471**, 766 (2011).
[28] T. Kimura, T. Goto, H. Shintani, K. Ishizaka, T. Arima, and Y. Tokura, Nature (London) **426**, 55 (2003).
[29] N. Hur, S. Park, P. A. Sharma, J. S. Ahn, S. Guha, and S.-W. Cheong, Nature (London) **429**, 392 (2004).
[30] S.-W. Cheong and M. Mostovoy, Nat. Mater. **6**, 13 (2007).
[31] R. Ramesh and N. A. Spaldin, Nat. Mater. **6**, 21 (2007).
[32] I. E. Dzyaloshinskii, Sov. Phys. JETP **10**, 628 (1959).
[33] D. N. Astrov, Sov. Phys. JETP **11**, 708 (1960).
[34] M. Fiebig, J. Phys. D: Appl. Phys. **38**, R123 (2005).
[35] S. Park, Y. J. Choi, C. L. Zhang, and S.-W. Cheong, Phys. Rev. Lett. **98**, 057601 (2007).
[36] F. Schrettle, S. Krohns, P. Lunkenheimer, J. Hemberger, N. Büttgen, H. A. Krug von Nidda, A. V. Prokofiev, and A. Loidl, Phys. Rev. B **77**, 144101 (2008).
[37] A. Ruff *et al.*, J. Phys.: Condens. Matter **26**, 485901 (2014).
[38] T. Kimura, Y. Sekio, H. Nakamura, T. Siegrist, and A. P. Ramirez, Nat. Mater. **7**, 291 (2008).
[39] S. Seki, X. Yu, S. Ishiwata, and Y. Tokura, Science **336**, 198 (2012).
[40] E. Ruff, P. Lunkenheimer, A. Loidl, H. Berger, and S. Krohns, Sci. Rep. **5**, 15025 (2015).
[41] G. Dhalenne, A. Revcolevshi, M. Ain, B. Hennion, G. Andre, and G. Parette, Cryst. Prop. Prep. **36-38**, 11 (1991).
[42] A. C. Komarek, T. Taetz, M. T. Fernández-Díaz, D. M. Trots, A. Moller, and M. Braden, Phys. Rev. B **79**, 104425 (2009).
[43] L. Zhao, M. T. Fernández-Díaz, L. H. Tjeng, and A. C. Komarek, Sci. Adv. **2**, e1600353 (2016).
[44] R. Szymczak, H. Szymczak, A. V. Zalessky, and A. A. Bush, Phys. Rev. B **50**, 3404 (1994).
[45] N. Mufti, G. R. Blake, M. Mostovoy, S. Riyadi, A. A. Nugroho, and T. T. M. Palstra, Phys. Rev. B **83**, 104416 (2011).
[46] K. Siratori, J. Akimitsu, E. Kita, and M. Nishi, J. Phys. Soc. Jpn. **48**, 1111 (1980).
[47] H. Murakawa, Y. Onose, K. Ohgushi, S. Ishiwata, and Y. Tokura, J. Phys. Soc. Jpn. **77**, 043709 (2008).